https://doi.org/10.33472/AFJBS.6.13.2024.1211-1228

African Journal of Biological Sciences

Journal homepage: http://www.afjbs.com

Research Paper Open Access

Intranasal Delivery of Ropinirole-Loaded Chitosan Nanoparticles in Thermoresponsive In-Situ Gel: A Novel Approach for Enhanced Parkinson's Disease Treatment and Neuroprotection

Christina Das[1*], Muruganantham V[2]

[1*]Research Scholar, Vinayaka Mission's College of Pharmacy, Salem, Tamil Nadu, India.

[2]Professor, Vinayaka Mission's College of Pharmacy, Salem, Tamil Nadu, India.

Corresponding Email: [1*]christe.das@gmail.com

Article Info

Volume 6, Issue 13, July 2024

Received: 02 June 2024

Accepted: 30 June 2024

Published: 24 July 2024

doi: 10.33472/AFJBS.6.13.2024.1211-1228

ABSTRACT:

Objective: To develop and assess a new formulation of Ropinirole-loaded chitosan nanoparticles incorporated into an in-situ gel for treating Parkinson's disease (PD), focusing on its properties and therapeutic potential.

Methods: Physicochemical properties, drug-excipient compatibility, and thermal behavior of the nanoparticles were characterized using FTIR and DSC analysis. These nanoparticles were combined with a poloxamer-based in-situ gelling solution for nasal delivery. The formulation's therapeutic efficacy was tested in haloperidol-induced PD Wistar rats.

Results: Successful development of ropinirole-loaded chitosan nanoparticles with desired properties was achieved. Incorporating them into an in-situ gel enhanced administration ease and nasal cavity retention. In PD rat models, the formulation reduced brain lipid peroxidation and TBARS levels, with highest GHS content in the in-situ gel-treated groups. Improved motor coordination, especially with the in-situ gel formulation, was observed in the catalepsy test.

Conclusion: The intranasal delivery of Ropinirole-loaded chitosan nanoparticles in an in-situ gel exhibits stability, mucus penetration, and potential blood-brain barrier permeation for PD treatment. These results indicate a promising avenue for developing patient-friendly PD therapies. Further research into intranasal RNP formulations could enhance therapeutic outcomes in PD management.

Keywords: Ropinirole, Parkinson's Disease, Nanoparticles, In-Situ Gel, Animal Study.

1. INTRODUCTION

Parkinson's disease, which affects over 6 million individuals worldwide, is currently the second most common neurological illness [1,2]. According to epidemiological statistics, men and the old population have a higher chance of getting PD, with an estimated prevalence of 4% in men over the age of 80 [3]. The primary neuropathological mechanisms behind PD include the degeneration of dopaminergic neurons in the substantia study oxidative stress, neuro-inflammation, and α-synuclein aggregation leading to Lewy neurite production [4]. The condition often manifests clinically as motor symptoms, such as stiffness, bradykinesia, tremor, and speech impairments. Apart from their motor symptoms, people with PD may also experience non-motor symptoms include depression, constipation, gastrointestinal disorders, and idiopathic rapid eye movement (REM) sleep disorder. These non-motor symptoms primarily arise before the beginning of PD and subsequently evolve with cognitive impairment and motor symptoms as the illness progresses into the advanced stage [5]. Patients with PD will eventually see a decline in both their mental and quality of life due to these symptoms.

As PD is a complicated neurological disorder with no known treatment, people can manage their condition by reducing their symptoms, which can improve their cognitive abilities. Various therapeutic techniques have been developed to address PD. The majority of these symptomatic treatment options involve neuroprotective therapies, which include the use of dopaminergic supplements (e.g., Levodopa, Carbidopa), dopaminergic agonists (e.g., Pramipexole, Ropinirole), COMT inhibitors (e.g., Entacapone, Tolcapone), MAO-B inhibitors (e.g., Rasagiline, Selegiline), etc. [6]. Ropinirole (Requip®, GlaxoSmithKline) is an FDA-approved non-ergoline dopamine D2 agonist that is commonly used in clinics for the treatment of early and severe PD [7,8]. When administered as monotherapy or in conjunction with levodopa, ropinirole has been shown in several clinical studies to significantly improve PD signs and symptoms [9]. However, due to first-pass metabolism and the blood-brain barrier (BBB), the pharmacological effectiveness of its standard formulation produced via oral administration is limited [10]. As a result, during the last ten years, a lot of research has been done to create innovative formulations that use nanocarriers and improved delivery techniques to carry ropinirole to the brain effectively and selectively.

Intranasal drug administration has received a lot of interest in recent years for brain drug delivery because of its capacity to boost drug bioavailability in the brain by bypassing the BBB, avoiding first-pass metabolism, and gastrointestinal enzymatic degradation of the medication [11]. Moreover, the intranasal route has the potential to offer less systemic toxicity, improved therapeutic impact, and a quicker rate of drug absorption. Furthermore, intra-nasal administration is a painless and patient-friendly method for PD patients due to its simplicity of self-administration [12]. The intranasal mode of administration is not without its drawbacks, though, including limited nasal residence duration, poor penetration of hydrophilic medicines, enzymatic drug degradation in the nasal cavity, and nasal mucociliary clearance [13]. Several researchers have successfully overcome these issues by formulating nano-carrier-based intranasal formulations [14,15]. Through their easy penetration of the nasal mucosal barrier, ability to withstand enzymatic destruction, and ability to enter the brain directly through the olfactory route, the nano-carriers will improve the absorption of the medicine [16]. The enhanced efficacy of treating PF has been established by researchers using several nano-systems, including polymeric, lipid, nano-emulsion, and nano-hydrogel nanoparticles, for the intranasal delivery of the ropinirole. Mucoadhesive polymeric nanoparticle-based *in situ* gels have been investigated for Ropinirole–intranasal administration in an effort to further enhance the nasal residence time and the absorption time [17-19]. These nanoparticle-based *in situ* gel systems can help manage the prolonged release drugs by establishing more intimate contact with the nasal mucosa, which can speed up drug absorption. In this study, we developed a new

Ropinirole-loaded chitosan nanoparticles-based *in situ* gel formulation and tested its pharmacodynamics in haloperidol-induced PD Wistar rats [20.21].

2. MATERIALS AND METHODS

Materials

Nice Chemicals, India, provided the ropinirole, chitosan polymer, and sodium tripolyphosphate (TPP). Poloxamer 407, Poloxamer 188 was procured from Yarrow chem products. The remaining substances were all of analytical quality and produced locally by vendors.

Pre-Formulation Studies

Drug Excipient Compatibility Analysis by FTIR:

The drug-excipient compatibility was investigated using Fourier-transform Infrared FTIR Spectroscopy (Alpha II, Bruker, Germany). The sample was made by dispersing Ropinirole in KBr in a 1:3 ratio and compressing it to a pellet at a pressure of 600 kg/cm2. The resultant pellet was examined in a spectrophotometer between 400 and 4000 cm-1.

Thermal Analysis of the Formulation

The DSC thermograms of pure API or mixes were obtained using a differential scanning calorimeter (DSC 60, Schimadzu) in order to determine the melting points. One to three milligram samples that were precisely weighed were placed into solid aluminum pans and sealed, then crimped. As a guide, an empty sealed aluminum pan was retained. The thermograms were produced by heating at a rate of 20°C per minute while purging with dry nitrogen at a rate of 20 mL/min.

Formulation of Chitosan-Based Ropinirole Nanoparticles

According to the scientific literature, chitosan nanoparticles were formulated via ionic cross-linking of the negatively charged polymer chitosan using TPP. Two solutions of chitosan (0.05 mg/mL in 1% acetic acid) and TPP (1% TPP) were made in 40 ml each using ultra-purified water [22]. 40 mL of the previously indicated chitosan solution was combined with 2000 uL of a 1% TPP solution, and the mixture was magnetically stirred at 200 RPM. Nanoparticles were produced via the interaction of chitosan in solution with TPP. These nanoparticles were used in an additional investigation [23]. RNP was formed as a result of the cross-linking procedure. A combination of 20 millilitres of a 0.06 mg/ml chitosan solution and 3 millilitres of a 2 mg/ml ropinirole solution was made. To the drug-polymer mixture, 800 uL of 1% TPP is added while magnetically stirring at 200 rpm. This resulted in the formation of Nanoparticles which were stored and characterized in the final step [24].

Physicochemical Properties of Formulated Nanoparticles

Particle Size and Size Distribution of Nanoparticles

The PDI and particle size of formulations were assessed using the DLS technique (Zeta sizer, Malvern, UK). After samples were placed in a disposable cuvette and filled to a depth of 1 cm, light scattering measurements were taken at right angles at a temperature of 25±2 °C.

Drug Entrapment Efficiency of Nanoparticles

The entrapment effectiveness of RNP is determined using the ultracentrifugation technique by estimating the quantity of API that was not entrapped. The EE was estimated by centrifuging formulations for 25 minutes at 4°C at 15000 RPM [25].

Drug Release Studies of Nanoparticles

For activation, a 14KD molecular cut-off mini dialysis kit (Pur-A-Lyzer TM, Sigma Aldrich) was soaked in the buffer. Three milliliters of RNP dispersion are added to 100 milliliters of simulated nasal fluid (SNF) that has been maintained at 37 ±0.5 °C in a beaker. With a temperature-controlled magnetic stirrer, the setup was kept agitated at 50 revolutions per minute. Three millilitres samples were collected at predetermined intervals, and the content of ropinirole was measured at 250 nm using a UV-Visible spectrophotometer (Shimadzu 1800, Japan). After each sample, SNF is added to maintain sink conditions [26].

Drug Release Kinetics

To undertake preclinical drug research, data on drug release under mimicked physiological settings must be collected. The regulatory clearances and assessments of pharmaceuticals will also be based on these data. It is an increasingly common procedure when developing nano formulations to use *in vitro* approaches to anticipate drug release *in vivo*. Mathematical models may be used to predict the methods by which medications are released into the body, in addition to aiding in the development of formulations and controlled drug release systems. The use of *in vitro* drug release data to anticipate and define drug ingredient *in vivo* performance is therefore a critical step in the rational development of controlled release formulations, as evidenced by the fact that the above-mentioned conclusion may be derived [27]. The Zero-order, First-order, Korsmeyer-Peppas, and Higuchi Models were among the drug release kinetics models.

Preparation of Ropinirole Nanoparticle Loaded in-Situ Gel

Poloxamer 407 and poloxamer 188 were weighed as per formulation table 1 and added into 30 ml of Ropinirole Nano suspension to produce six different ratios of *in situ* gelling solution. The resultant mixture was stirred for 4 hours in a magnetic stirrer at a temperature below 100^0C using an ice bath.

Table 1: Parameters For In Situ Gel Preparation

Sl No	Formulation code	Poloxamer 407 (%)	Poloxamer 188 (%)	Ropinirole Nano suspension
1	F1	24	4.0	30 ml
2	F2	25	3.3	30 ml
3	F3	26	2.6	30 ml
4	F4	27	1.8	30 ml
5	F5	29	1.0	30 ml
6	F6	30	0.0	30 ml

Evaluation of in situ gel

Evaluation of Gelling: Visual observations were used to determine gelling. The point of gelling is defined as the complete cessation of flow. The solutions were heated in a water bath progressively until the gelling happened. The temperature was continually checked, the gelling temperature was recorded.

Determination of Viscosity

The rheological properties of the sample before and after gelling were determined by using a Brookfield viscometer DV -II+ Pro and a helipath spindle F96 at various RPMs and the results are noted.

Antiparkinson's Study of Nanoparticles

Animal Grouping

Six groups of rats, each with six numbers, were formed. The study was handled in the following manner: groups I and II were the normal and PD controls, respectively. Group III was given R (ropinirole), Group IV was given RC (ropinirole Chitosan Nano Formulation), Group V was given RCG (Ropinirole Chitosan Nano Formulation Gel) and Group VI was given the control formulation, RG (Ropinirole Gel formulation).

Pharmacodynamic Study

Haloperidol-induced PD Wistar rats were used in pharmacodynamic (PCD) tests using RP (ropinirole) loaded chitosan nanoparticles, matching hydrogel, and control formulations. PD was induced by intraperitoneal injection of 1 mg/kg of haloperidol [28].

Biochemical Studies

Tissue preparation

Following the induction of PD in the rats, the animals were put to euthanasia, and the striatum and substantia nigra were extracted from their brains. This was accomplished by slicing the brain, using a rat brain atlas as a guide, into coronal slices that were 1 mm thick. Striatum was homogenised at 10% (w/v) in a 0.01 M phosphate buffer (pH 7.0) for the enzymatic tests that followed. The post-mitochondrial supernatant (PMS) was isolated by centrifuging the homogenate for 20 minutes at 4°C at 11,000 rpm. The dopamine levels, TBARS (thiobarbituric acid reactive substances) levels, catalase activity, and the activity of the antioxidant enzyme GSH (glutathione) were all measured using this PMS.

Lipid Peroxidation

The lipid peroxide levels in the RP (Reference Product) from various formulations were determined using a previously established approach [29]. In brief, 200 µL of post-mitochondrial supernatant (PMS) was added to an Eppendorf tube and allowed to incubate for 60 minutes at 100 rpm in a water bath shaker at 37 ± 1 °C. In parallel, an additional 200 µL of PMS was incubated at 0 °C in a different Eppendorf tube. Both sets of samples (i.e., the ones at 0 °C and the one at 37 °C) received 400 µL of 0.67% TBA and 400 µL of 5% trichloroacetic acid after an hour of incubation. Following the transfer of the reaction mixture from the vial to the tube, the tube was centrifuged for 15 minutes at 1200 rpm. The supernatant that was obtained was then transferred to another tube and placed in a boiling water bath for 10 minutes. After the test tubes cooled, the colour absorbance at 535 nm was measured. The amount of lipid peroxidation was measured in nanomoles (nmol) of TBARS (thiobarbituric acid reactive substances) that were formed every hour per milligram (mg) of protein.

Assay for Reduced Glutathione Content (GSH)

The 200 µL of post-mitochondrial supernatant (PMS) was precipitated by mixing it with 200 µL of 4% sulfosalicylic acid. After being kept at 4 °C for at least an hour, these samples were centrifuged for 15 minutes at 4 °C at 1200 revolutions per minute. A filtered aliquot (10%, w/v) in 100 µL of 1.7 mL of phosphate buffer (0.1 M, pH 7.4) and 200 µL of DTNB (dithiobisnitrobenzoic acid) (4 mg/mL in phosphate buffer, 0.1 M, pH 7.4) made up the assay combination, which had a total volume of 2 mL. At 412 nm, the yellow color that this combination produced was available for measurement right away [30].

Determination of Catalase Activity
We measured the catalase activity using the procedure described by Coliborne in 1985. To summarise, the test combination had a total volume of 3.0 mL and contained 200 µL of phosphate buffer (0.1 M, pH 7.4), 950 µL of hydrogen peroxide (0.019 M), and 50 µL of post-mitochondrial supernatant (PMS). We measured variations in absorbance at 240 nm. The measurement of catalase activity was expressed in terms of nanomoles of H2O2 ingested per minute per milligram of protein.

Animal Testing
In this investigation, male Wistar rats (Harlan, France) weighing between 220 and 230 g at the start of the trial were employed. The animals were kept in typical laboratory settings with a light-dark cycle at 22 ± 2 C. Water and food were given freely. The European Communities Council Directive of November 24, 1986 (86/609/EEC) on the use and care of animals for experimental procedures was followed in the conduct of all the research. All reasonable steps were taken to reduce suffering, and an attempt was made to utilise as few animals as possible. Therapeutic interventions and categorization of animals prior to administration, the neurotoxic substance rotenone (RT) was dissolved in sunflower oil in order to induce PD in the animal model of PD. The animals were categorized into five groups, with each group consisting of eight animals (Scheme 1). The user did not provide any text.
Group 1 (G1): The group that serves as a control group. Animals are being given the vehicles, specifically sunflower oil.
Group 2 (G2): Animals 6 receiving radiation therapy (2 mg/kg/day) for 35 days.
Group 3 (G3) of animals received a dose of RT (2 mg/kg/d) for a duration of 35 days. Additionally, the amount of R was reduced to 1 mg/kg/d RP every 3 days starting from day 15.
Group 4 (G4) consisted of animals that received a dosage of RT (2 mg/kg/d) for a duration of 35 days, along with a dosage of RCin saline (1 mg/kg/d) starting from day 15.
Group 5 (G5) of animals received a dose of RT (2 mg/kg/d) for a duration of 35 days, and RCG in saline (1 mg/kg/d) starting from day 15.
Group 6 (G6): Animals 6 were administered RT (2 mg/kg/d) for a duration of 35 days, and RG in saline (1 mg/kg/d) starting from day 15.

The animals were beheaded using a guillotine after a period of 35 days.
Assessment of Body Weight Animals were weighed on predetermined days (day 1, 5, 10, 15, 20, 25, 30, and 35) in order to assess changes that occurred throughout the course of the research.

Behavioural Testing
Catalepsy test
The grid and bar catalepsy test was conducted on days 15, 22, 29, and 36. When an animal first exhibited movement, the time it took for the movement to occur was recorded as descending latency. The experimental animals were hung by all four limbs on a vertical grid measuring 25.5 by 44 cm, with a gap of 1 cm between each wire. The animals were placed in a position where both of their front paws were resting on a bar that was 10 cm above and parallel to the base during the bar portion of the test. The rats were partially raising themselves, with both forepaws positioned on the bar. Latency was observed during paw removal. For both tests, the maximum descent delay was set at 180 seconds. Each animal underwent a triple catalepsy test [31,32].

Akinesia Test.
The animals' latency (measured in seconds) to move all four limbs was established by performing the akinesia test at pre-arranged dates (days 15, 22, 29, and 36). When delay surpassed 180 s, the test was declared over. The animals were placed on an elevated platform (100 cm) for five minutes in order to acclimatise them to the test (100 - 150 cm). The animal's time taken to move each of its four limbs was then timed. For every animal, akinesia testing was carried out in triplicate [33].

Rotarod Test
The animals' motor balance and coordination were assessed using a rotarod device (Rotarod LE 8200; Letica Scientific Instruments, Barcelona, Spain) that had falling sensors and automated timers. Previously, the animals were trained to use the rotarod for one minute every day for five days in a row. Animals were put on the rotarod at a steady pace of 12 revolutions per minute for the test, and the latency—or amount of time in seconds—that it took for the animals to fall off the rod was noted [34]. When latency above 300 s, the test was declared over. Three sets of rotarod tests were conducted on days 15, 22, 29, and 36.
In order to assess the novel formulation's therapeutic efficacy, behavioural, histological, and immunochemical tests were carried out. As behavioural tests can be converted into clinical performance in human situations, they aid in the investigation of the symptom-relieving benefits of therapy [35].
In our investigation, 14.3% of the animals receiving RT experienced mortality, while the control group of animals did not experience any deaths. Using RT dissolved in DMSO (2.75–3 mg/kg/d), other scientists [36] reported 10% animal death that occurred soon (minutes) after injection. In their evaluation of RT at two dose levels (2 and 2.5 mg/kg), [37] found that at the highest dose, mortality was 46.7%, whereas at the lower dose, it was only 6.7%. Since we used a lower dose of RT (2 mg/kg/d) and a less toxic vehicle (sunflower oil) for our trial, none of the animals in our case died soon after injection.

3. RESULTS AND DISCUSSION

Pre-Formulation Studies
Drug Excipient Compatibility Analysis by FTIR:
Possible interactions between API and formulation excipients are predicted by FT-IR data. Table 2 shows the FTIR spectra of the crosslinkers TPP and RNP, as well as the chitosan polymer and ropinirole. Alcoholic OH group stretches were found at 3624.81, 3686.24, and 3732.06 cm^{-1} for chitosan. First and second-degree N-H bond elongation was seen at 2870.87 and 3284.12 cm^{-1}, C-H elongation and bending was recorded at 893.81, 1373.78, and 416.50 cm^{-1}, and C-O-C bridge elongation was found at 1149.34 cm^{-1}. The C=O stretch of Gama lactam was also detected at 1643.97 cm^{-1}. With ropinirole, the amine N-H stretch was detected at wavelengths of 2983.53, 2969.45, and 3070.06 cm^{-1}.

Table 2: The infrared spectroscopy data for various functional groups in Chitosan, Ropinirole, and TPP compounds. Wavelengths (cm^{-1}) correspond to specific vibrational modes observed in each functional group

Compound	Functional group	Wavelengths (cm^{-1})
Chitosan	Alcoholic OH	3624.81, 3686.24, 3732.06
	C=O stretch of Gama lactam	1643.97
	C-H elongation and bending	893.81, 1373.78, 416.50
	N-H bond elongation	2870.87 (first degree), 3284.12 (second degree)

	C-O-C bridge elongation	1149.34
Ropinirole	Amine N-H stretch	2983.53, 2969.45, 3070.06
	C-H stretch	1391.16, 1456.03, 1760.21
	C=O stretch	1702.22
TPP	C-H stretch and bending	891.9, 1372.81, 1414.60
	N-H stretch	2871.21 (first degree), 3284.1 (second degree)
	C-O-C bridge stretch	1150.12
	P-O-P bridge	1209.50 (antisymmetric stretching)
	P = O stretching	1126.72
	PO2 group	1956.64 (symmetric), 883.35 (antisymmetric)

The FTIR measurements demonstrate that there are no chemical linkages between the preparation's polymer and ropinirole. The polymer and API are hence compatible.

Thermal analysis of the formulation

A prominent endothermic peak at 254.22°C was seen in Ropinirole's DSC thermograms. The DSC curve for chitosan showed an exothermic peak at 306.79°C and an endothermic peak at 128.32°C. An endothermic peak was seen at 125.72°C by TPP DSC thermographs. Ropinirole-chitosan DSC thermographs showed a peak at 296.07 °C.

A decrease in the drug's melting point was seen in the DSC thermogram of the formulation of ropinirole and RNP, perhaps indicating a decrease in the compound's crystalline nature.

Physicochemical Properties of Formulated Nanoparticles

Particle Size and Size Distribution of Nanoparticles

Bare chitosan nanoparticles had an average particle size of 139.40 nm and a Polydispersity index (PDI) of 0.328. The zeta potential of the bare chitosan nanoparticle was found to be -20.0 mV.

The average particle size and PDI for RNP were 156.70 and 0.241, respectively. The zeta potential of RNP was -11 mV.

The optimized formulation can penetrate the mucus layer and the blood-brain barrier to reach its target site since its particle size is in the nano-size range.

Zeta potential for the final optimized formulations of chitosan NP and RNP is found to be -23.0 mV and -27.6 mV, respectively. A zeta potential of ±30 mV is ideal. It implies that the formulation is stable.

The negatively charged mucus membrane may repel the RNP if it has a negative zeta potential. The nanoparticles' adhesion and interaction with the mucosal surface may be restricted by this repellence, which might affect their penetration and bioavailability. Chitosan is a recognized mucoadhesive material that can improve drug absorption by facilitating interaction with the mucosal membrane. But other factors, like as composition, surface modification of the nanoparticles, and sizes less than 200 nm, can also influence their behavior when administered through the nasal cavity [38].

Drug Entrapment Efficiency of Nanoparticles

RNP formulation showed a 90.5% drug entrapment efficiency.

Drug Release Studies of Nanoparticles

The drug release profile of RNP was systematically investigated in a pH 7.4 medium over 12 hours. The results revealed that approximately 86.3% of the drug was released during this timeframe.

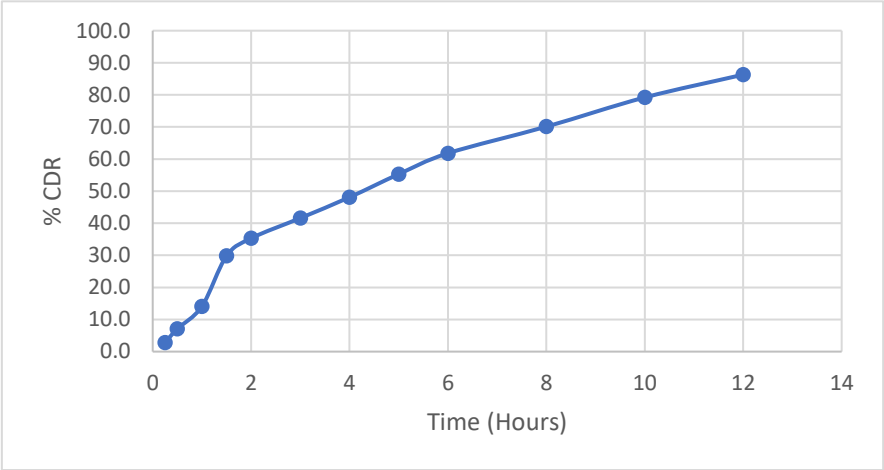

Fig. 1: The release of ropinirole from RNP at pH 7.4

Drug Release Kinetics

Several other in vitro kinetics models were examined, and it was determined that the first-order model, shown in Table 3, best suited the in vitro data.

Table 3: Drug release kinetic modelling data of drug release

Plot	Slope	R2 value	n	Observed Drug release Mechanism
Zero-order	6.8250	0.9159		
1st order	-0.0681	**0.9917**		First-order drug release
Higuchi	0.0347	**0.9818**		Fickian Diffusion controlled Drug release
Kosmeyer peppas	1.2505	0.9584	1.1281	

Higuchi's model illustrates ropinirole release from an insoluble matrix as the square root of a time-dependent process based on Fickian diffusion [39,40]. Through a comparison of the correlation coefficients of each model, the model that was deemed most equivalent to the release data was selected. Diffusion-controlled drug release from Chitosan nanoparticles was suggested by the higher R2 values (0.98 for the Higuchi model).

Evaluation of in Situ Gel

Determination of Gelling

Observations of gelling determination are noted in Table 4 from which F2 found to have gelling at 34°C is taken into consideration for additional analysis.

Table 4: Gelling temperatures of various formulations

Sl No	Formulation code	Gelling temperature
1	F1	38°C ± 0.40
2	**F2**	**34**°C ± 0.235

3	F3	31°C ± 0.816
4	F4	28°C ± 0.380
5	F5	25°C ± 0.41
6	F6	22°C ± 0.0115

The in situ gels underwent evaluation for gelation temperature, and it was observed that F2 exhibited gelation at a nasal temperature of **34**°C ± 0.235 conducive to the nasal delivery of RNP. Subsequently, F2 was further assessed for viscosity both before and after gelation.

Determination of Viscosity

The Results of the viscosity measurement of F2 formulation are recorded in Table 5.

Table 5: Results of viscosity measurement

Torque (%)	Viscosity (cp)	RPM
Before gelling		
1.9	8 ± 0.010	12
1.2	25 ± 0.011	6
2.1	54 ± 0.004	3
After gelling		
96.2	480 ± 0.012	3

Antiparkinson's study of nanoparticles

Pharmacodynamic Study

PCD studies were carried out in haloperidol-induced PD Wistar rats. To validate the motor impairment in rats following a 1 mg/kg IP injection of haloperidol, preliminary investigations were carried out. Haloperidol at this dosage has the potential to cause moderate catalepsy and motor instability. The animals' induction of PD was verified using the rotarod and standard bar tests. Although the exact origin of PD is still unknown, evidence suggests that a number of factors, including extensive oxidative stress, the production of free radicals, hereditary vulnerability, and programmed cell death, may be involved in the disease's development. The disease's neuropathology is predicated on the death of brain cells in the dopaminergic nigrostriatal tract, which lowers striatal dopamine levels. The animal groups received formulations according to the experimental protocol. One hour after haloperidol was administered, the animals were killed, brain tissue was taken, and striatum was used to make PMS. Estimates were made for GSH, TBARS, catalase activity, and DA levels.

Biochemical Studies

Lipid Peroxidation

The study revealed that the TBARS content in the negative control group G1 was 2.81 ± 0.40 nmol/mg protein. This is considerably ($p < 0.001$) lower than the TBARS content in the haloperidol-induced control group G2 (9.43 ± 0.25 nmol/mg protein). A reduction in the amount of TBARS (4.95 ± 0.82 nmol/mg protein, 4.42 ± 0.67 nmol/mg, and 4.58 ± 0.38 nmol/mg protein) was seen in the haloperidol-induced treatment group G3, G4, and G6, although it was still considerably ($p < 0.001$) greater than that of the negative control group. Interestingly, haloperidol-induced group 5 showed a substantial (p 0.001) drop in TBARS (3.43 0.75 nmol/mg protein) as compared to the haloperidol-induced control group (Figure 2), although the data were not statistically different from the negative control group ($p > 0.05$).

Fig. 2: Estimation of lipid peroxidation levels (*n=3)

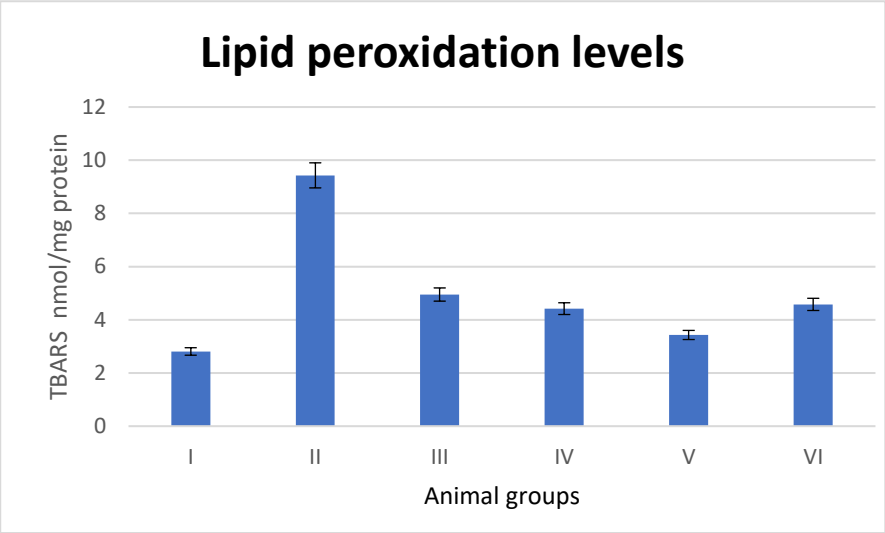

Assay for Reduced Glutathione Content (GSH)

When compared to the negative control group 1, which had a GSH content of 14.56 ± 0.28 µmol/mg protein, the haloperidol-induced group G2 had a considerably lower GSH content ($p < 0.001$), with 2.49 ± 0.38 µmol/mg protein. The GSH content rose to 5.28 ± 0.49 µmol/mg protein in G3, 6.34 ± 0.36 µmol/mg protein on G4, and 5.76 ± 0.34 µmol/mg protein in G6 after the group's haloperidol-induced therapy, although it was still much lower than in group 1. As anticipated, the GSH content (12.57 ± 1.15 µmol/mg protein) of the haloperidol-induced group 5 was significantly higher ($p < 0.001$) than that of the haloperidol-induced control group G2, and the values did not differ significantly ($p > 0.05$) from the negative control group G1 (Figure 3).

Fig. 3: Assay of GSH

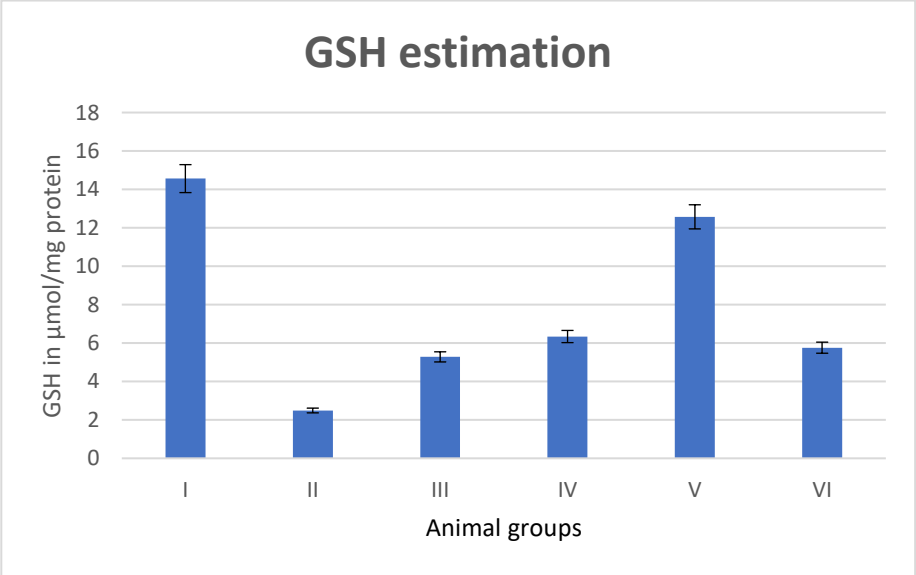

Determination of Catalase Activity

The CAT content in the negative control group G1 was 151.7 ±12.25 nmolH2O2/min/mg protein, which was significantly (p 0.001) greater than in the haloperidol-induced control group G2 (47.66 9.07 nmolH2O2/min/mg protein). The G3 CAT content was seen to be 64.83 ± 7.97 nmolH2O2/min/mg protein in the haloperidol-induced group, while the G4 and G6 CAT contents were reported to be 52.34 ± 7.64 nmolH2O2/min/mg protein and 61.58 ± 9.07 nmolH2O2/min/mg protein. Nevertheless, the results were considerably ($p < 0.001$) lower than the negative control group. As anticipated, group 5's haloperidol-induced treatment resulted in a significantly higher CAT content (137.66 ± 13.05 nmolH2O2/min/mg protein) than group 2 (Figure 4). However, the values did not differ significantly ($p > 0.05$) from the negative control group, suggesting that G5 treatment in conjunction with levodopa demonstrated protective antioxidant activity.

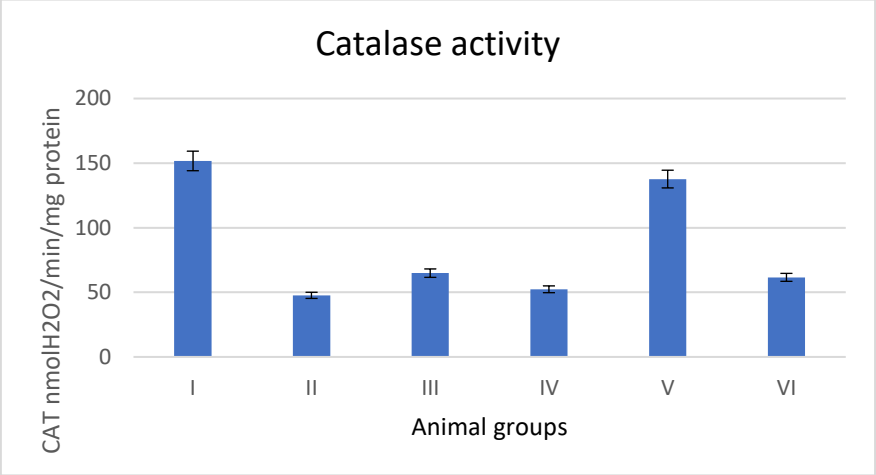

Fig. 4: Estimation of catalase activity

It has also been previously documented that lipid peroxide and GSH activities, as well as associated enzymes, have an inverse connection in PD [41]. A decrease in GSH can make it more difficult to remove H2O2 from the body and encourage the production of OH, which raises the free radical load and causes oxidative stress, which impairs homeostasis. One may reasonably assume that GSH depletion causes lipid peroxide to be released, which in turn causes nigrostriatal neurons to degenerate and release DA [42]. The beneficial benefits of the created lipid Nano formulations and associated hydrogel formulations in the successful treatment of PD were proven by the rise in GSH content and decrease in the extent of lipid peroxide. Comparable outcomes were also noted when RP was formulated as a Nano emulsion gel for the treatment of PD [43].

Animal testing At intervals of 0, 5, 10, 15, 20, 25, 30 and 35 days, the evolution of body weight was noted (Figure 5). Throughout the trial, the animals in control group G1, which is represented by those receiving the vehicles (sunflower oil), gained weight gradually and steadily; non-significant differences (p >.05) were noted when compared to the other groups. During the first two weeks of treatment, animals given G2 experienced a very minor rise in weight, which was likely caused by the onset of neurodegeneration. Compared to group G2, animals treated with groups G3, G4, G5, and G6 showed a consistent improvement in their weight increase after 15 days.

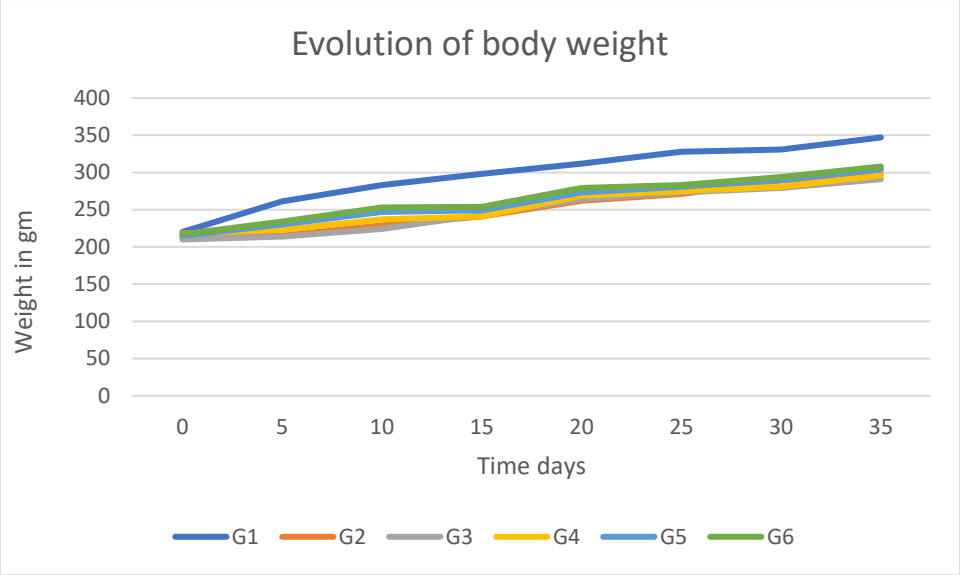

Fig. 5: Body weight and time profile

Catalepsy Test

Figure 6 displays the results of the catalepsy test (gird and bar) at 15, 20, 28, and 35 days. In the control animals given both vehicles—sunflower oil—non-significant changes ($p > .05$) were found. Nonetheless, RT-treated mice (G2) and other group animals were found to vary statistically significantly (42) . In both the grid and bar tests of catalepsy, the neurotoxic in G3 caused an increase in latency, which RP reversed. Beginning on day 22, which is seven days after RP was first administered, there was a noticeable improvement in latency following the administration of RP in saline and RP in nanoform enclosed within NPs G4. Yet, group G5 produced the greatest results at the end of the trial period (35 days), indicating the potential utility of the newly designed nanosystem gel for (ropinirole). Latency in G6 was almost identical to that in G3.

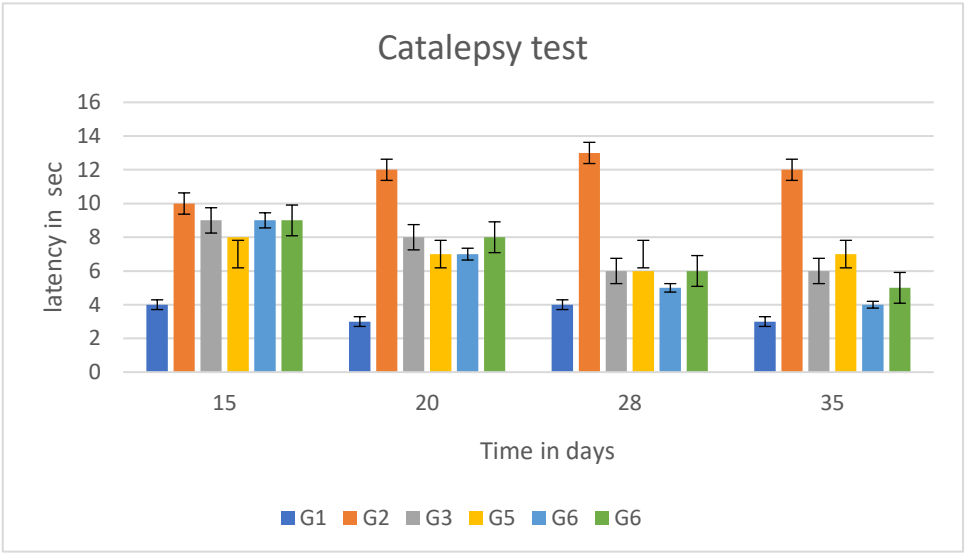

Fig. 6: Catalepsy test (*Mean of 3 trials)

Akinesia Test

The akinesia test findings are displayed in Figure 7, where non-significant changes were observed in the control groups (G1) 43). When RT was administered to group G2, descent latency was significantly delayed in comparison to group G3, with group G2's latency values being greater than those of G3. Similar to the catalepsy test, group G5's receipt of RP-loaded NPs gel produced the best results. Group G5's latency values at the study's conclusion (35 days) were comparable to those of the control subgroups (G1). At the end of the study, however, latency values from the administration of RP in saline (1 mg/kg/d) were statistically substantially higher than those from the control group (G1).

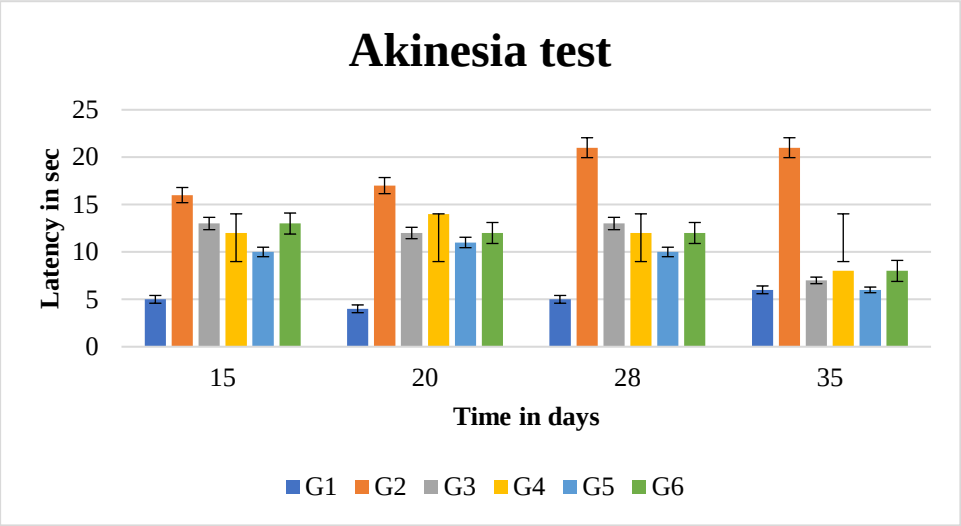

Fig. 7: Akinesia test (*Mean of 3 trials)

Rotarod Test

The rotarod test, which is particularly sensitive in identifying cerebellar impairment, is frequently used to assess mice' motor coordination. Many factors, including stiffness, bradykinesia, and lack of coordination, influence rotarod performance. Days 15, 22, 29, and 35 were used for this test (44). Compared to control group G1, the animals' time spent on the rotarod was significantly reduced after receiving RT (Fig. 8).

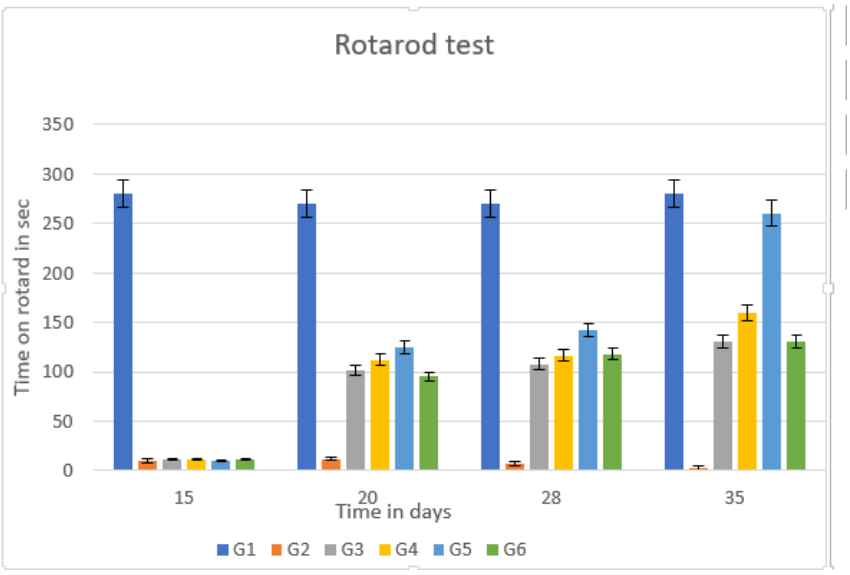

Fig. 8: Rotarod test (*Mean of 3 trials)

The distinct variations suggest that the neurotoxic is causing neurodegeneration. Recent research has suggested that both chronic subcutaneous injections of RT and local injections of RT into the substantia nigra pars compacta (SNpc) cause abnormal behavior on the rotarod [44]. Motor coordination was enhanced by the administration of RP (G3, G4, and G5), with group G5 achieving the greatest outcomes. By the end of the research, these animals' outcomes were comparable to those of the control group.

4. CONCLUSION

In conclusion, the intranasal approach presents a promising avenue for addressing one of the most prevalent neurological conditions in today's world—Parkinson's disease. Leveraging the advantages of needle-free drug delivery, minimal physical intervention, and direct access to the central nervous system (CNS), the intranasal administration of the RNP formulation emerges as a potential strategy to enhance the targeted transport of active pharmaceutical ingredients (APIs) for PD therapy.

By avoiding the blood-brain barrier, intranasal delivery offers the opportunity to elevate drug concentrations within the brain, mitigating systemic adverse effects and allowing for less frequent dosing. This holds significant implications for improving the efficacy and safety profile of PD treatment. Further exploration and development of intranasal RNP formulations could pave the way for innovative and patient-friendly therapeutic interventions in the management of this challenging neurological condition.

Acknowledgement

We would like to express my sincere gratitude to Vinayaka Mission’s College of Pharmacy, Salem, Tamil Nadu, India, for providing the necessary facilities and support for conducting this research as part of my PhD work. Furthermore, we extend our heartfelt appreciation to Nazareth College of Pharmacy, Othera, Thiruvalla, Kerala, India, for their invaluable contributions to this work.

Funding

Nil

Authors Contributions

The contributions from each author are equal.

Conflict of Interest

The authors state that there are no real, potential, or perceived conflicts of interest in this research.

5. REFERENCES

1. Bloem BR, Okun MS, Klein C. Parkinson’s Disease. The Lancet. 2021; 397 (10291): 2284-2303. doi:10.1016/S0140-6736(21)00218.
2. Mohan R, Kayalvizhi R. Ramanathan J, Shanmugam, Archana R. Impact of caloric vestibular stimulation on co-ordination in parkinson disease induced mice”. International Journal of Pharmacy and Pharmaceutical Sciences. 2022; 14(10): 46-49, doi:10.22159/ijpps.2022v14i10.45523.
3. Marino BL, de Souza LR, Sousa KP, Ferreira JV, Padilha EC, da Silva CHTP, Taft CA, Hage Melim LIS. Parkinson’s Disease: A Review from Pathophysiology to Treatment.

Mini-Reviews in Medicinal Chemistry. 2020; 20 (9): 754-767. doi: 10.2174/1389557519666191104110908.

4. Zhu B, Yin D, Zhao H, Zhang L. The Immunology of Parkinson's Disease. Semin Immunopathol. 2022; 44 (5): 659-672. doi:10.1007/s00281-022-00947-3.
5. Jagdish Chand, Amarjith Thiyyar Kandy, Kaveri Prasad, Jinu Mathew, Farhath Sherin, Gomathy Subramanian. In silico, preparation and in vitro studies of benzylidene-based hydroxy benzyl urea derivatives as free radical scavengers in parkinson's disease. International Journal of Applied Pharmaceutics. 2024; 16(3): 217-224.
6. Vijiaratnam N, Simuni T, Bandmann O, Morris HR. Foltynie, T. Progress towards Therapies for Disease Modification in Parkinson's Disease. Lancet Neurol. 2021; 20(7): 559-572. doi:10.1016/S1474-4422(21)00061-2.
7. Adler CH, Sethi KD, Hauser RA, Davis TL, Hammerstad JP, Bertoni J, Taylor RL, Sanchez Ramos, J. O'Brien CF. Ropinirole for the Treatment of Early Parkinson's Disease. Neurology 1997; 49 (2): 393-399. doi;10.1212/WNL.49.2.393.
8. Schrag A, Keens J, Warner J. Ropinirole for the Treatment of Tremor in Early Parkinson's Disease. Eur J Neurol. 2002; 9 (3): 253-257. doi:10.1046/j.1468-1331.2002.00392.
9. Pahwa R, Lyons KE, Hauser RA. Ropinirole Therapy for Parkinson's Disease. Expert Rev Neurother. 2004; 4 (4): 581-588. doi:10.1586/14737175.4.4.581.
10. Kaye CM, Nicholls B. Clinical Pharmacokinetics of Ropinirole. Clin Pharmacokinet. 2000; 39 (4); 243-254. doi:10.2165/00003088-200039040-00001.
11. Mona Ibrahim El-Assal, Dalia Samuel. Optimization of rivastigmine chitosan nanoparticles for neurodegenerative Alzheimer; in vitro and ex vivo characterizations. International Journal of Pharmacy and Pharmaceutical Sciences. 2022; 14(1): 17-27. doi:10.22159/ijpps.2022v14i1.43145.
12. Kapoor A, Hafeez A, Kushwaha P. Nanocarrier Mediated Intranasal Drug Delivery Systems for the Management of Parkinsonism: A Review. Curr Drug Deliv. 2023; doi:10.2174/1567201820666230523114259.
13. Keller LA, Merkel O, Popp A. Intranasal Drug Delivery: Opportunities and Toxicologic Challenges during Drug Development. Drug Deliv Transl Res. 2022; 12 (4): 735-757. doi:10.1007/s13346-020-00891-5.
14. Kumar Katual M, Singh GL, Harikumar S. Recent Advancements in Ropinirole Hydrochloride Embedded Nano-Techniques in Parkinson's Treatment. Panacea Journal of Medical Sciences. 2020; 9 (3): 92-103. doi:10.18231/j.pjms.2019.023.
15. Bhalothia C, Nagda G. Nanotherapeutics a Promising Approach for Treatment of Parkinson's Disease. Mater Today Proc. 2022; 69: A1-A13. doi:10.1016/j.matpr.2022.10.311.
16. Barcia E, Boeva L, García-García L, Slowing K, Fernández-Carballido A, Casanova Y, Negro S. Nanotechnology-Based Drug Delivery of Ropinirole for Parkinson's Disease. Drug Deliv. 2017; 24 (1): 1112-1123. doi:10.1080/10717544.2017.1359862.
17. Dudhipala N, Gorre T. Neuroprotective Effect of Ropinirole Lipid Nanoparticles Enriched Hydrogel for Parkinson's Disease: In Vitro, Ex Vivo, Pharmacokinetic and Pharmacodynamic Evaluation. Pharmaceutics. 2020; 12 (5): 448. doi:10.3390/pharmaceutics12050448.
18. Sita VG, Jadhav D, Vavia P. Niosomes for Nose-to-Brain Delivery of Bromocriptine: Formulation Development, Efficacy Evaluation and Toxicity Profiling. J Drug Deliv Sci Technol. 2020; 58: 101791. doi:10.1016/j.jddst.2020.101791.

19. Mustafa G, Ahuja A, Al Rohaimi AH, Muslim S, Hassan AA, Baboota S, Ali J. Nano-Ropinirole for the Management of Parkinsonism: Blood–Brain Pharmacokinetics and Carrier Localization. Expert Rev Neurother. 2015; 15 (6); 695-710. doi:10.1586/14737175.2015.1036743.
20. Jafarieh O, Md S, Ali M, Baboota S, Sahni JK, Kumari B, Bhatnagar A, Ali J. Design, Characterization, and Evaluation of Intranasal Delivery of Ropinirole-Loaded Mucoadhesive Nanoparticles for Brain Targeting. Drug Dev Ind Pharm. 2015; 41 (10): 1674-1681. doi:10.3109/03639045.2014.991400.
21. Dudhipala N, Gorre T. Neuroprotective Effect of Ropinirole Lipid Nanoparticles Enriched Hydrogel for Parkinson's Disease: In Vitro, Ex Vivo, Pharmacokinetic and Pharmacodynamic Evaluation. Pharmaceutics. 2020; 12 (5): 448. doi:10.3390/pharmaceutics12050448.
22. Tanasale MFJDP, Bijang CM, Rumpakwara E. Preparation of Chitosan with Various Molecular Weight and Its Effect on Depolymerization of Chitosan with Hydrogen Peroxide Using Conventional Technique. Int J Chemtech Res. 2019; 12 (01): 112-120. doi: 10.20902/IJCTR.2019.120113.
23. Balde A, Hasan A, Joshi I, Nazeer RA. Preparation and Optimization of Chitosan Nanoparticles from Discarded Squilla (Carinosquilla Multicarinata) Shells for the Delivery of Anti-Inflammatory Drug: Diclofenac. J Air Waste Manage Assoc. 2020; 70 (12): 1227-1235. doi:10.1080/10962247.2020.1727588.
24. Jafarieh O, Md S, Ali M, Baboota S, Sahni JK, Kumari B, Bhatnagar A, Ali J. Design, Characterization, and Evaluation of Intranasal Delivery of Ropinirole-Loaded Mucoadhesive Nanoparticles for Brain Targeting. Drug Dev Ind Pharm. 2015; 41 (10): 1674-1681. doi:10.3109/03639045.2014.991400.
25. Rinaldi F, Hanieh P, Chan L, Angeloni L, Passeri D, Rossi M, Wang J, Imbriano A, Caraf M, Marianecci C. Chitosan Glutamate-Coated Niosomes: A Proposal for Nose-to-Brain Delivery. Pharmaceutics. 2018; 10 (2): 38. doi:10.3390/pharmaceutics10020038.
26. Galgatte UC, Kumbhar AB, Chaudhari PD. Development of in itu Gel for Nasal Delivery: Design, Optimization, in vitro and in vivo Evaluation. Drug Deliv. 2014; 21 (1): 62-73. doi:10.3109/10717544.2013.849778.
27. Herdiana Y, Wathoni N, Shamsuddin S, Muchtaridi M. Drug Release Study of the Chitosan-Based Nanoparticles. Heliyon. 2022; 8 (1): 08674. doi:10.1016/j.heliyon.2021.e08674.
28. Dudhipala N, Gorre T. Neuroprotective Effect of Ropinirole Lipid Nanoparticles Enriched Hydrogel for Parkinson's Disease: In vitro, Ex Vivo, Pharmacokinetic and Pharmacodynamic Evaluation. Pharmaceutics. 2020; 12 (5): 448. doi:10.3390/pharmaceutics12050448.
29. Robert A, Handbook Methods For Oxygen Radical Research. e book edition 2017. doi://www.routledge.com/Handbook-Methods-For-Oxygen-Radical-Research-1stedition/ Greenwald/p/book/9781315893822.
30. Azeem A, Talegaonkar S, Negi LM, Ahmad FJ, Khar RK, Iqbal Z. Oil Based Nanocarrier System for Transdermal Delivery of Ropinirole: A Mechanistic, Pharmacokinetic and Biochemical Investigation. Int J Pharm. 2012; 422 (1–2): 436–444. doi: 10.1016/j.ijpharm.2011.10.039.
31. Sofroniew MV, Vinters HV. Astrocytes: Biology and Pathology. Acta Neuropathol. 2010; 119 (1): 7-35. doi:10.1007/S00401-009-0619-8/FIGURES/9.

32. Jost W H, Angersbach D. Ropinirole, a Non-Ergoline Dopamine Agonist. CNS Drug Rev. 2005; 11 (3): 253–272. doi:10.1111/j.1527-3458.2005.tb00046.x.
33. Jost WH, Buhmann C, Fuchs G, Greulich W, Hummel S, Korchounov A, Mungersdorf M. Schwarz M, Spiegel-Meixensberger M. Initial Experience with Ropinirole PR (Prolonged Release). J Neurol. 2008; 255 (S5): 60-63. doi:10.1007/s00415-008-5008.
34. Kasinathan N, Jagani HV, Alex AT, Volety SM, Venkata Rao J. Strategies for Drug Delivery to the Central Nervous System by Systemic Route. Drug Deliv. 2015; 22 (3): 243-257. doi:10.3109/10717544.2013.878858.
35. Sindhu KM, Saravanan KS, Mohanakumar KP. Behavioral Differences in a Rotenone-Induced Hemiparkinsonian Rat Model Developed Following Intranigral or Median Forebrain Bundle Infusion. Brain Res. 2005; 1051 (1–2): 25-34. doi:10.1016/j.brainres.2005.05.051.
36. Cannon JR, Tapias V, Na HM, Honick AS, Drolet RE, Greenamyre JTA. Highly Reproducible Rotenone Model of Parkinson's Disease. Neurobiol Dis. 2009; 34 (2): 279-290. Doi:10.1016/j.nbd.2009.01.016.
37. Zhang ZN, Zhang JS, Xiang J, Yu ZH, Zhang W, Cai M, Li XT, Wu T, Li WW, Cai DF. Subcutaneous Rotenone Rat Model of Parkinson's Disease: Dose Exploration Study. Brain Res. 2017; 1655: 104-113. doi:10.1016/j.brainres.2016.11.020.
38. Mikusova V, Mikus P. Advances in Chitosan Based Nanoparticles for Drug Delivery. Int J Mol Sci. 2021;22 (17): 9652. doi:10.3390/ijms22179652.
39. Paul DR. Elaborations on the Higuchi Model for Drug Delivery. Int J Pharm. 2011;418 (1): 13-17. doi:10.1016/j.ijpharm.2010.10.037.
40. Bayer IS. Controlled Drug Release from Nanoengineered Polysaccharides. Pharmaceutics. 2023; 15 (5): 1364. doi:10.3390/pharmaceutics15051364.
41. Kalia LV, Lang AE. Parkinson's Disease. The Lancet. 2015; 386 (9996): 896-912. doi:10.1016/S0140-6736(14)61393-3.
42. Dauer W, Przedborski S. Parkinson's Disease: Mechanisms and Models. Neuron. 2003; 39 (6): 889-909. doi:10.1016/S0896-6273(03)00568-3.
43. Uversky VN. Neurotoxicant Induced Animal Models of Parkinsons Disease: Understanding the Role of Rotenone, Maneb and Paraquat in Neurodegeneration. Cell Tissue Res. 2004; 318 (1): 225-241. doi:10.1007/s00441-004-0937-z.
44. Wrangel, C von, Schwabe K, John N, Krauss JK, Alam M. The Rotenone-Induced Rat Model of Parkinson's Disease: Behavioral and Electrophysiological Findings. Behavioural brain research. 2015; 279: 52-61. doi:10.1016/J.BBR.2014.11.002.